

# LBM for Rarefied Gas Flows

Seminar Lattice Boltzmann Methods:  
Theory, Implementation and Applications

Gerasimos Chourdakis  
Fakulät für Informatik  
Technische Universität München  
Email: gerasimos.chourdakis@tum.de

June 11, 2015

We divide different flow regimes and we explain the main weaknesses of the continuous methods like Navier-Stokes equations. We pose problems that appear while passing from the continuum to the slip and then to the transient regime, together with some solutions for the lattice Boltzmann method, mainly by using a Multiple-Relaxation-Times collision operator and by choosing a suitable slip-velocity boundary condition. Finally, we present a stochastic approach for virtual wall collisions, in order to deal with free-flowing particles and model a way of thermalisation for rarefied gas flows, where the intermolecular collisions are rare.

## 1 Introduction

If someone tried to sell a Computational Fluid Dynamics software, based on the Lattice Boltzmann Method to, e.g., a naval industry, he/she would probably have to face the argument “but we successfully use a software that solves the Navier-Stokes equations for many years now!”. Indeed, the Navier-Stokes(-Fourier) equations are the main tool of the classical approach to the CFD. Yet, they bring with them some important *assumptions*, that restrict their usage in a limited range of applications. The fundamental assumption they pose is the *continuity of the matter*. In the case of the naval industry, that has to solve problems mainly in the scales we can see and touch, the matter appears to be continuous, so the application of the NSE is usually legit.

Modern engineers, though, need to design devices far smaller than ships, in which fluids or gases need e.g. to flow through pipes smaller than hair. Such devices are for example micropumps, micromotors and other Micro-Electro-Mechanical Systems [2]. Microflows and nanoflows are also faced in Chemical Engineering and relevant fields, in devices like microreactors [5], particle separators [2] or in materials with nanopores,

like in the shale-gas extraction process. The continuity assumption breaks down in such scales, as e.g. the molecules of the used gases are so rare that interact mainly with the walls and less with other particles. The same holds also for very low-pressure scenarios as in aero-astronautics applications [7].

In such problems, LBM can be applied, though the Bhatnagar-Gross-Krook approach, with Single-Relaxation-Time and bounce-back boundary conditions, poses some problems because of the rare collisions of the molecules, that is assumed to be the main mechanism that leads to an equilibrium (thermalisation). Various modifications have been proposed to solve these problems and some of them are presented in this work.

## 2 Rarefied gas flows

### 2.1 The Knudsen number

For gases we define their *Mean Free Path* as the average distance that the molecules of this gas are traveling without taking part in collisions. The MFP of a hard-sphere gas in thermodynamic equilibrium is given by the equation:

$$\lambda = \frac{1}{\sqrt{2}\pi \cdot n_g \cdot d^2} \quad (1)$$

where  $d$  is the mean molecular diameter and  $n_g$  the number density of the gas [9]. Referring to the mean molecular spacing as  $\delta$ ,  $n_g = \delta^{-3}$ . For air at atmospheric conditions ( $T = 298$  K,  $p = 1$  atm),  $\lambda_{\text{air}} = 6.111 \cdot 10^{-8}$  m while for the (lighter and smaller) helium  $\lambda_{\text{He}} = 17.651 \cdot 10^{-8}$  m [2].

Knowing the MFP of a gas we can compute the *Knudsen number* for a given scale. This is defined as the ratio of the MFP to the characteristic length  $L_0$  of the geometry:

$$\text{Kn} := \frac{\lambda}{L_0} \quad (2)$$

In complex geometries, a local Knudsen number can be chosen to solve the problem of deciding about the characteristic length. We can also relate the Knudsen number to the Mach and Reynolds numbers:

$$\text{Kn} = \frac{\lambda}{L_0} \cdot \sqrt{\frac{\pi\gamma}{2}} \cdot \frac{\text{Ma}}{\text{Re}} \quad (3)$$

where  $\gamma := c_p/c_V$  is the specific heat capacity ratio of the gas [9].

### 2.2 Division of the gas flow regimes

The Knudsen number can be used to divide different *flow regimes* and a rough, empirical classification can be found in figure 1, though it has been shown that Knudsen number is not the only parameter that needs to be taken into account [1]. The region  $\text{Kn} < 10^{-2}$  (or  $\text{Kn} < 10^{-3}$ , as more recently suggested) is referred to as the *continuum regime*, in which

all the required assumptions hold, so that the application of the Navier-Stokes equations with the usual no-slip boundary conditions is valid. The other part of the range, where  $\text{Kn} > 10$ , corresponds to the *free molecular regime*. In this area, the molecules almost do not collide with each other. In between, the gas flow may belong to the *slip-flow regime* ( $10^{-2} < \text{Kn} < 10^{-1}$ ) or to the *transition regime* ( $10^{-1} < \text{Kn} < 10$ ). Navier-Stokes and other continuous methods may be applied in these regimes only using special boundary conditions or higher-order extensions, like the Burnett equations or other models, that usually derive from a truncated Chapman-Enskog expansion of the LBE [9].

Which regimes are mainly of practical interest? The term *Rarefied Gas Flows* usually refers to the slip-flow and the transition regime. As an example,  $\text{Kn} = 1$  for air is achieved around length scale  $L_0 = 65$  nm. In some applications, different scales and flow regimes may be paired (*mixed flow regimes*), leading to the need of studying transport phenomena in a wide Knudsen range [2].

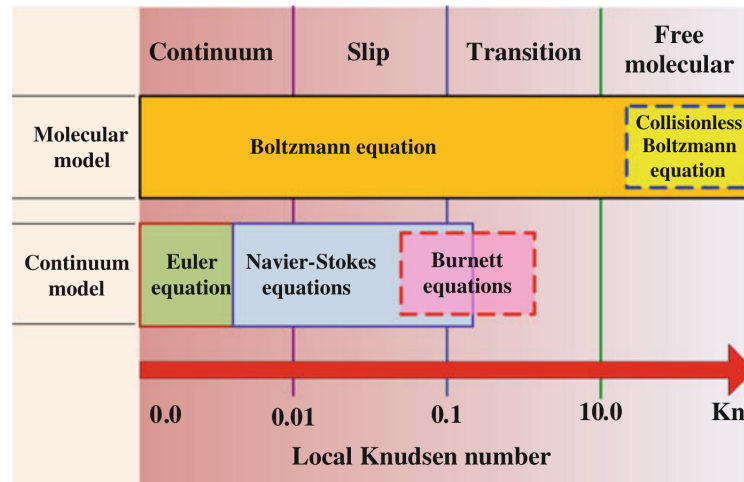


Figure 1: Division of the gas flow regimes in relation to the Knudsen number, along with the limits of different CFD approaches. [9]

### 2.3 Where the continuous methods break

The Navier-Stokes equations describe the conservation of mass and momentum in the system. Adding the conservation of energy, we have the Navier-Stokes-Fourier equations that require the following assumptions [1]:

**Newtonian Framework** The fluid motion has to be unrelativistic, i.e. the characteristic velocity has to be much smaller than the speed of light. This assumption is usually satisfied in the problems of our interest. It wouldn't hold in the case of the flow of e.g. high-energy particles or the motion of stars/galaxies.

**Continuum approximation** The fluid is infinitely divisible. This means that properties like the pressure, the velocity and the shear stress can be defined locally as averages between neighboring cells of a mesh. This assumption depends on the Knudsen number and it mainly does *not* hold in our problems.

**Thermodynamic equilibrium** The particles of the system have enough time to reach an equilibrium, by colliding with each other and relaxing the values of their properties. This depends on the frequency of the collisions and thus the Knudsen number.

It is suggested that the ratio  $L_0/\delta$  should be greater than 100 in order to achieve statistically stable estimate of macroscopic quantities (limit of molecular chaos) and thus to assume continuity [1]. Starting from the continuum regime, an increase in the Knudsen number breaks the thermodynamic equilibrium assumption at around  $\text{Kn} = 10^{-3}$ , as temperature jumps start to occur between the molecules and the walls, forcing the gas to “slip” on the wall, i.e., the velocity near the wall cannot be assumed as zero and the mass flux increases. In the slip regime, the continuous methods can still be applied, combined with slip-velocity and temperature-jump boundary conditions. In the transition regime, a non-linear stress-strain relationship is observed for the fluid near the walls. This area, that has width of a few MFP, is called “*Knudsen layer*”. The continuum assumption breaks down and the NSF equations cannot be applied, while the lattice Boltzmann method must be extended.

### 3 Extending the LBM to the slip flow regime

The lattice Boltzmann BGK model with bounce-back boundary conditions has been used to simulate pressure-driven microchannel flows because of their simplicity and low computational cost. It is, though, discussed that this approach has some problems: the boundary conditions used depend on the viscosity, the “slip-velocity” observed is actually a numerical artifact (as it depends on the grid resolution) and it is constant at the walls, without depending on the Knudsen number [8]. Various alternative approaches have been proposed in order to deal with these problems, using a Two-Relaxation-Time [6] or a Multiple-Relaxation-Time [8] collision operator, various slip boundary conditions [9] and other ideas like virtual-wall collisions [7].

#### 3.1 Multiple-Relaxation-Time

Verhaeghe et al. [8] present some deficiencies of the Single-Relaxation-Time BGK approximation with bounce-back boundary conditions, noting that it mainly does not have enough freedom to adjust higher-order discretization errors. They also show that this approach fails qualitatively for a microchannel flow of  $\text{Kn} = 0.194$ , compared to the Direct Simulation Monte Carlo results. In order to deal with these problems, they successfully use a MRT collision operator, something that also other authors report [3, 5, 6].

We remind here that the general form of the lattice Boltzmann equation is:

$$\mathbf{f}(\mathbf{r}_j + \mathbf{c}\delta_t, t + \delta_t) = \mathbf{f}(\mathbf{r}_j, t) + \mathbf{\Omega}[\mathbf{f}(\mathbf{r}_j, t)] + \mathbf{F}(\mathbf{r}_j, t) \quad (4)$$

where  $\mathbf{f}$  is the vector of the particle distribution functions in each direction,  $\mathbf{r}_j$  the lattice,  $\mathbf{c}$  the discrete velocity set of the particles,  $\mathbf{\Omega}$  the collision operator and  $\mathbf{F}$  the external forcing term. In the MRT case, the collision operator is:

$$\mathbf{\Omega} = -\mathbf{M}^{-1} \cdot \mathbf{S} \cdot [\mathbf{m} - \mathbf{m}^{(\text{eq})}] , \text{ where } \mathbf{m} = \mathbf{M} \cdot \mathbf{f} \quad (5)$$

where  $\mathbf{m}$  is the moment space (and  $\mathbf{m}^{(\text{eq})}$  their equilibria),  $\mathbf{S}$  a positive-definite matrix of the relaxation rates and  $\mathbf{M}$  the matrix that transforms  $\mathbf{f}$  to their moments [8]. In this formulation, every moment relaxes with a different rate and with appropriate selection of the  $\mathbf{S}$ , the MRT method can be reduced to a TRT scheme or the BGK approximation.

### 3.2 Boundary conditions

The analytic solution of the lattice Boltzmann equation for the incompressible Poiseuille flow is, in dimensionless form:

$$\tilde{u}(\tilde{y}) = 4\tilde{y}(1 - \tilde{y}) + \tilde{U}_{\text{slip}} \quad (6)$$

where  $\tilde{u} := (u + G\delta_t/2)/U_{\text{max}}$ ,  $G := |\nabla p/\rho|$  (acceleration due to a constant pressure gradient),  $\tilde{U}_{\text{slip}} := U_{\text{slip}}/U_{\text{max}}$  and  $\tilde{y} := (j-1/2)/N_y$ .  $N_y$  is the number of cells per width-direction, identified by the index  $j$ . The slip velocity term depends on the boundary conditions and the elements  $\tau_i$  of the relaxation matrix  $\mathbf{S}$  [8].

The theory of the pressure-driven flow through a long microchannel requires that, on the wall, the perpendicular velocity term vanishes and the tangential term is given by a velocity model that, in the slip regime, can be of first-order, as e.g.:

$$u|_{\text{wall}} = \sigma \text{Kn} L_0 \partial_y u_{\text{wall}}, \quad \sigma := (2 - \sigma_\nu)/\sigma_\nu \quad (7)$$

where  $\sigma_\nu \in (0, 1]$  is the tangential momentum accommodation coefficient [8]. Verhaeghe et al. take  $\sigma_\nu = 1$  and Barber and Emerson [1] provide more details on the TMAC and its estimation. In the case of a long microchannel, with length/height ratio  $L/H \gg 1$ , the characteristic length is set as  $L_0 = H$ .

In the corresponding literature, the following boundary conditions may be found: bounce-back, diffusive, specular reflective and combinations of them [8].

#### 3.2.1 Bounce-back boundary conditions

According to these conditions, that correspond to very smooth surfaces, when the molecules collide with the walls, their momentum is reversed:

$$f_i(t_{n+1}) = f_i^*(t_n) \quad (8)$$

In this context, the slip velocity can be set as [8]:

$$U_{\text{slip}}^{\text{B}} = \frac{1}{4} \left( \frac{8}{\tau_s} - \frac{8 - \tau_s}{2 - \tau_s} \right) G \delta_t \quad (9)$$

where  $\tau_s, \tau_q$  are the relaxation rates for the stresses and the energy fluxes, respectively. For a boundary parallel to the lattice axis,  $U_{\text{slip}}^{\text{B}} = 0$  if and only if:

$$\tau_q = \frac{8(2 - \tau_s)}{(8 - \tau_s)} \quad (10)$$

### 3.2.2 Diffusive boundary conditions

In the case of non-smooth surfaces, the molecules are reflected to random directions (diffusive reflection). The diffusive boundary conditions set:

$$f_i = \frac{\sum_{\mathbf{c}_k} |\mathbf{c}_k \cdot \hat{\mathbf{n}}| f_k^*}{\sum_{\mathbf{c}_k} |\mathbf{c}_k \cdot \hat{\mathbf{n}}| f_k^{(\text{eq})}(\rho_{\text{wall}}, \mathbf{u}_{\text{wall}})} f_i^{(\text{eq})}(\rho_{\text{wall}}, \mathbf{u}_{\text{wall}}) := f_i^{\text{D}}, \quad \mathbf{c}_k \cdot \hat{\mathbf{n}} < 0 \quad (11)$$

where  $\hat{\mathbf{n}}$  is the normal to the wall unit vector,  $\mathbf{c}_k$  are incidental velocities defined by  $\mathbf{c}_k \cdot \hat{\mathbf{n}} < 0$  and  $\rho_{\text{wall}}$  and  $\mathbf{u}_{\text{wall}}$  are the density and velocity at the wall, respectively. Using these boundary conditions, we get for the slip velocity [8]:

$$U_{\text{slip}}^{\text{D}} = U_{\text{slip}}^{\text{B}} + \frac{3}{2} N_y G \delta_t = U_{\text{slip}}^{\text{B}} + \frac{3}{2} \frac{L_0 G}{c}, \quad c := \delta_x / \delta_t \quad (12)$$

### 3.2.3 Diffusive bounce-back boundary conditions

Combining the previous two boundary conditions, we get the following general form:

$$f_i(t_{n+1}) = \beta f_i^*(t_n) + (1 - \beta) f_i^{\text{D}}(t_n), \quad \beta \in [0, 1] \quad (13)$$

$$U_{\text{slip}}^{\text{BD}} = U_{\text{slip}}^{\text{B}} + \frac{3(1 - \beta)}{2(1 + \beta)} N_y G \delta_t = U_{\text{slip}}^{\text{B}} + \frac{3(1 - \beta)}{2(1 + \beta)} \frac{L_0 G}{c} \quad (14)$$

that can be reduced in one of the previous pure diffusive or bounce-back boundary conditions. Verhaeghe et al. [8] show that, assuming the first-order slip velocity of eq. 7 with  $U_{\text{slip}}^{\text{B}} = 0$  it holds for the  $\beta$ :

$$\beta = \frac{3\mu - \text{Kn} L_0 c \bar{\rho}_{\text{out}}}{3\mu + \text{Kn} L_0 c \bar{\rho}_{\text{out}}} \quad (15)$$

In the equation 15, an assumption is hidden: the viscosity  $\mu$  must be constant, something that doesn't hold in the transition regime. Verhaeghe et al. present nice results for the slip regime using MRT, the first-order model of eq. 7 and DBB boundary conditions, although they point out that this is not valid in higher Knudsen numbers.

### 3.2.4 Specular reflective bounce-back boundary conditions

The specular reflective boundary conditions (also known as “free-slip”) maintain the tangential momentum and reverse the perpendicular one. Combining them with the bounce-back boundary conditions we get similarly [8]:

$$U_{\text{slip}}^{\text{BR}} = U_{\text{slip}}^{\text{B}} + \frac{3(1 - \beta)}{2\beta} N_y G \delta_t = U_{\text{slip}}^{\text{B}} + \frac{3(1 - \beta)}{2\beta} \frac{L_0 G}{c} \quad (16)$$

## 4 The LBM in the transition flow regime

In a bounded system, the mean free path of the molecules near the walls is shorter, because the molecules collide both with other gas molecules and the solid. For hard-sphere gases, the bulk viscosity is given by the Chapman-Enskog theory of dilute gases as:

$$\mu_0 = \frac{5}{6} \sqrt{\frac{2\pi kT}{m}} \rho \lambda \approx 0.49 \rho \bar{c} \lambda \quad (17)$$

where  $\bar{c}$  is the mean thermal speed [4]. From equation 17 it is clear that a shorter MFP will decrease the viscosity. This change of viscosity in the Knudsen layer makes it non-constant and there is a need to define an *effective viscosity*. Michalis et al. [4] propose and verify the following form for this:

$$\mu_e = \mu_0 \frac{1}{1 + \alpha \text{Kn}} \quad (18)$$

and they calculate the Bosanquet parameter  $\alpha = 2$  for a wide range of Kn. The *effective mean free path* is then given by [3]:

$$\lambda_e = \frac{\mu_e}{p} \cdot \sqrt{\frac{\pi RT}{2}} \quad (19)$$

In the transient flow regime, it has been reported that first-order slip velocity models do not reproduce the observed results very accurately [1]. For this, various higher-order models have been proposed [9]. Various authors (e.g. [3, 5]) use a general second-order slip-velocity boundary condition:

$$U_{\text{slip}} = A_1 \sigma_\nu \lambda \frac{\partial u}{\partial y} \Big|_{\text{wall}} - A_2 \lambda^2 \frac{\partial^2 u}{\partial y^2} \Big|_{\text{wall}}, \quad \sigma_\nu = (2 - \sigma)/\sigma \quad (20)$$

There are various suggestions for the slip coefficients  $A_1$ ,  $A_2$  in the literature and extended tables are provided e.g. by Zhang et al. [9]. The same equation with different parameters  $B_1$ ,  $B_2$  can be applied also for the effective mean path  $\lambda_e$ .

As in the slip regime, Multiple-Relaxation-Time LBM is usually suggested. Li et al. set:

$$\tau_s = \frac{1}{2} + \sqrt{\frac{6}{\pi}} \frac{N \text{Kn}}{(1 + \alpha \text{Kn})}, \quad N = H/\delta_x \quad (21)$$

$$\tau_q = \frac{1}{2} + \frac{3 + 4\pi \tilde{\tau}_s^2 B_2}{16 \tilde{\tau}_s}, \quad \tilde{\tau}_s = \tau_s - 0.5 \quad (22)$$

For the diffusive bounce-back boundary conditions, in analogy to eq. 15,  $\beta$  is chosen as [3]:

$$\beta = \frac{1}{1 + B_1 \sigma_\nu \sqrt{\pi/6}} \quad (23)$$

## 5 A stochastic model for finite Knudsen numbers

Toschi and Succi [7] have proposed a stochastic model that works well for intermediate Knudsen numbers, as verified for a long microchannel. In their article, they focus on the problem that appears when trying to map a continuous direction space to a finite set of directions. In particular, they note that molecules that were going to travel in a direction slightly different than the (parallel to the lattice) flow direction, and collide with the wall after some time, are actually mapped to a direction in which they will never take part in a collision with the solid boundaries. This case is shown in figure 2.

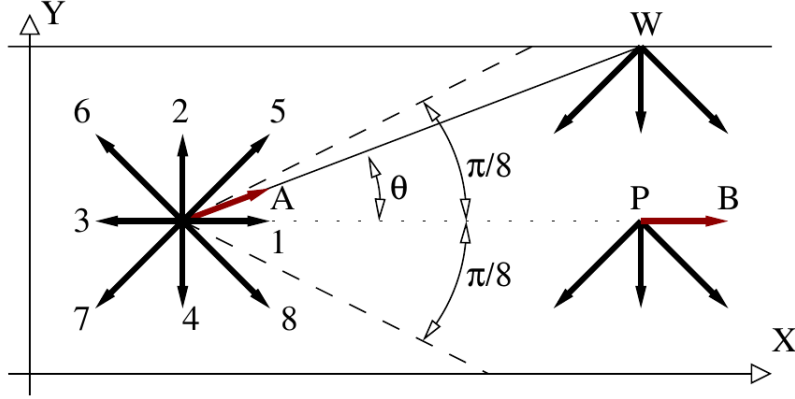


Figure 2: All the molecules that were going to travel within the  $-\pi/8 < \theta < \pi/8$  range are actually mapped to a single direction. Because this direction is parallel to the flow, and because the intermolecular collisions are rare, these molecules will never collide with the walls and they will continue accelerating. [7]

Because of the external forcing (i.e. a pressure gradient), an accelerating beam is created. Remember that, in high Knudsen number regions, the particles relax their properties mainly by interacting with the wall. To solve this problem, Toschi and Succi introduce a probability distribution for the direction after the collision, they use a virtual-wall-collision mechanism and they try the normal bounce-back and the Ansumali-Karlin boundary conditions. The latter ones re-inject molecules from the wall, in order to maintain the local equilibrium in respect to wall speed and temperature.

In order to model *virtual wall collisions*, they assign a *virtual speed*  $A$  ( $u_x, u_y$ ) =  $c \cdot (\cos \theta, \sin \theta)$  with  $\theta$  uniformly distributed in  $[-\pi/8, \pi/8]$  and they assume that the collisions follow a Poisson distribution. In this context, they define the probability of virtual wall collision as the probability to skip intermolecular collisions before hitting the wall, multiplied by the probability to collide with the wall in a time step:

$$p(x, y; t) = \exp(-1/\text{Kn}) \cdot \left( 1 - \exp \left( - \frac{c \cdot dt \cdot \sin(\theta(x, y))}{H} \right) \right) \quad (24)$$



This probability vanishes for very small Knudsen numbers (continuum regime) or for very small angles (direction parallel to the flow).

After colliding with e.g. the upper boundary (as in fig. 2), the particle distribution functions become:

$$\begin{aligned} f'_1 &= f_1(1-p) \quad , \quad f'_{7,8} = f_{7,8} + pf_1/6 \quad , \quad f'_4 = f_4 + 4pf_1/6 \\ f'_3 &= f_3(1-p) \quad , \quad f'_{5,6} = f_{5,6} + pf_3/6 \quad , \quad f'_2 = f_2 + 4pf_3/6 \end{aligned}$$

where  $\{1/6, 4/6, 1/6\}$  correspond to the weights of the nine-speed lattice scheme. Notice the different signs between the functions 1,3 and the other PDFs. With this formulation, momentum is re-distributed from the directions parallel to the walls to the other directions. This allows the system to relax towards a (non-local) equilibrium even for higher Knudsen numbers.

The authors test their model with Single-Relaxation-Time collision and apply both bounce-back and Ansumali-Karlin boundary conditions for Knudsen numbers up to 30 and for Mach number 0.03. They observe a minimum in mass flow at  $\text{Kn} \approx 1$ , something that is physical and is referred to as “*Knudsen paradox*”, but both BC overestimate this minimum. In general, the authors receive better results with Ansumali-Karlin boundary conditions, in accordance with prior predictions, especially in lower-Knudsen regions.

## 6 Conclusion

In this work we saw a division of flow regimes according to the Knudsen number, we described the problems that start to appear as the Knudsen number increases and we tried to present some ways to overcome the limitations and extend the lattice Boltzmann method up to the transition flow regime. We found out that Multiple-Relaxation-Time collision operators are mainly suggested, as the well-spread BGK approximation with one parameter is not able to resolve the Knudsen layer. A slip-velocity model is required for the boundary conditions that, in the case of the slip regime, can be of first-order, while higher-order models are required in the transition regime. Finally, a model that introduces virtual wall collisions to resolve the free-flowing “beams” is presented. All the presented approaches show good results for microchannel flows and it looks like lattice Boltzmann methods are the right tool to simulate rarefied gas flows. The free-molecular region is not so extensively explored by now concerning the application of LBM, but the available tools are for the moment sufficient for simulating a great range of application scenarios in microfluidics and nanofluidics.

## References

- [1] Robert Barber and David Emerson. Challenges in modeling Gas-Phase flow in microchannels: From slip to transition. *Heat Transfer Engineering*, 27(4):3–12, May 2006.

- [2] George Karniadakis, Ali Beskok, and Nayaran Aluru. *Microflows and nanoflows: fundamentals and simulation*. Interdisciplinary applied mathematics. Springer, 2005.
- [3] Q. Li, Y.L. He, G.H. Tang, and W.Q. Tao. Lattice Boltzmann modeling of microchannel flows in the transition flow regime. *Microfluidics and Nanofluidics*, 10(3):607–618, 2011.
- [4] Vasilis K. Michalis, Alexandros N. Kalarakis, Eugene D. Skouras, and Vasilis N. Burganos. Rarefaction effects on gas viscosity in the Knudsen transition regime. *Microfluidics and Nanofluidics*, 9(4-5):847–853, 2010.
- [5] Philipp Neumann and Till Rohrmann. Lattice boltzmann simulations in the Slip and Transition Flow Regime with the Peano Framework. *Open Journal of Fluid Dynamics*, 2(3):101–110, September 2012.
- [6] Ali Norouzi and JavadAbolfazli Esfahani. Two relaxation time lattice Boltzmann equation for high knudsen number flows using wall function approach. *Microfluidics and Nanofluidics*, 18(2):323–332, 2015.
- [7] F. Toschi and S. Succi. Lattice Boltzmann method at finite Knudsen numbers. *EPL (Europhysics Letters)*, 69(4):549, 2005.
- [8] Frederik Verhaeghe, Li-Shi Luo, and Bart Blanpain. Lattice Boltzmann modeling of microchannel flow in slip flow regime. *Journal of Computational Physics*, 228(1):147 – 157, 2009.
- [9] Wen-Ming Zhang, Guang Meng, and Xueyong Wei. A review on slip models for gas microflows. *Microfluidics and Nanofluidics*, 13(6):845–882, 2012.